JOURNAL OF Materials CHEMISTRY

The thermal stability of mixed phenylphosphonic acid/water intercalates of kaolin and halloysite. A TG–EGA and VT-DRIFTS study

Christopher Breen, Nigel D'Mello and Jack Yarwood

Materials Research Institute, Sheffield Hallam University, Howard Street, Sheffield, UK S1 1WB. E-mail: cbreen@shu.ac.uk

Received 15th May 2001, Accepted 1st November 2001
First published as an Advance Article on the web 4th January 2002

Phenylphosphonic acid undergoes a topotactic reation with the available hydroxyls on the gibbsite sheet of kaolin and halloysite during reflux in a water–acteone mixture at 70 °C. The reaction occurs much more rapidly with halloysite than with kaolin and the number of hydroxyls consumed is much higher for the halloysite than the kaolin. Variable temperature X-ray diffraction confirmed that the *d*-spacing for both kaolin–phenylphosphonic acid (KPPA) and halloysite–phenylphosphonic acid (HPPA) remained stable at 15.4 Å to temperatures greater than 450 °C. Variable temperature diffuse reflectance infrared Fourier transform spectroscopy (VT-DRIFTS) together with TG–MS analysis of the evolved gases confirmed that the phenyl ring was not thermally desorbed until after dehydroxylation began to take place. Moreover, these techniques showed that the complexes contained water which was desorbed near 150 °C. In addition VT-DRIFTS showed that this water was hydrogen bonded to the remaining surface hydroxyls on the gibbsite sheet resulting in a shift of the AlAlOH band from 934 to 885 cm^{-1} in both HPPA and KPPA. This band shifted back to 934 cm^{-1} when the hydrogen bonded water (characterised by an OH bending mode at 1643 cm^{-1} and an OH stretching mode at 3547 cm^{-1}) was thermally desorbed.

1 Introduction

Kaolin is a dioctahedral 1 : 1 layered clay mineral of structural formula $Al_2Si_2O_5(OH)_4$. Each layer consists of two sheets: a tetrahedral sheet in which silicon atoms are tetrahedrally coordinated by oxygen atoms; and an octahedral sheet where aluminium atoms are octahedrally coordinated to hydroxyl groups and shared apical oxygens from the silica tetrahedral sheet. Consequently, one side of each layer presents the siloxane surface arising from the bases of the silica tetrahedra whilst the other presents a surface of hydroxyl groups from the aluminium octahedra[1,2] Hydrogen bonding between these two surfaces imparts a significant cohesive energy between the layers which makes intercalation into kaolin difficult.[1,3–5]

Halloysite is a polytype of kaolin and differs mainly in the morphology of the crystals which are curved or rolled.[6,7] Halloysites occur naturally as expanded phases with *d*(001) spacings of 10.0 Å, compared with 7.2 Å for kaolin, as a result of the incorporation of water in the interlamellar space. Provided that the incoming molecule is polar, intercalation into halloysite is achieved more easily and rapidly than into kaolin. Indeed, this difference in the rate of intercalation is used to identify the presence of halloysite in admixtures with kaolin.[8,9]

Intercalation and hence the swelling of kaolin is achieved by using small polar molecules such as dimethyl sulfoxide (DMSO),[10–12] formamide[13–15] and hydrazine,[16–19] which are intercalated directly *via* hydrogen bonding to the aluminol surface. However, intercalation of other molecules may be achieved *via* replacement of an entraining agent such as dimethyl sulfoxide, water or acetone. Indeed, water-expanded kaolin is generally prepared *via* a DMSO intercalate and is then used to intercalate molecules such as pyridine,[20] amino acids,[21] and alkylamines.[22] Intercalated water is considered to weaken the hydrogen bonds between the layers, thus facilitating the introduction of another molecule. In some cases the use of water can even increase the amount of intercalated species in the kaolin gallery.[23]

Hydrated kaolins have also been used as an intermediate in the surface functionalisation of kaolins using alcohols to form ether linkages of the type Al–O–R where the organic R group replaces the proton on the hydroxyl (with evolution of water).[24,25] More recently, phenylphosphonic acid (PPA) has been reported to undergo such a topotactic reaction with the hydroxyl groups on the kaolin surface[26] in the same manner as the functionalisation of bayerite (aluminium hydroxide) with phosphonic acids.[27] The route to the kaolin–PPA intercalate involved refluxing kaolin in a water–acetone solution of PPA for several weeks to provide a fully intercalated material in which the PPA moiety was thermally stable to temperatures at or near the dehydroxylation temperature of the host mineral. Similar thermal stabilities have been recorded for PPA intercalated in layered double hydroxides (LDHs)[28] whereas in other cases little regard have been afforded this important property in LDHs,[29] layered γ-zirconium phosphate[30] and layered $AlH_3(PO_4)_2$.[31]

The aim of the present study is to complement and extend that of Wypych and co-workers[26] to determine whether the nature of the layered species has any influence on the ease and extent of intercalation and the thermal stability of the resulting product. Particular attention has been focussed on the use of evolved gas analysis (EGA) in combination with variable temperature diffuse reflectance infrared Fourier transform spectroscopy (VT-DRIFTS) to elucidate the nature of the interactions in PPA intercalates of the polytypes halloysite and kaolin. Moreover, this work contributes to the current debate concerning the role of water in kaolin organic intercalates and the effect on the infrared (and Raman) spectra of the hydroxyl stretching and deformation modes.[14,19,32]

DOI: 10.1039/b104254h

2 Experimental

2.1 Materials

The kaolin was provided by English China Clays International. The halloysite sample, from China, was provided by Dr Stephen Hillier of the Macauley Land Use Research Institute. Phenylphosphonic acid (98%) was obtained from Aldrich and used without further purification.

2.2 Apparatus

VT-DRIFTS was performed using a Mattson Polaris FTIR spectometer, a Graseby Selector™ DRIFTS accessory and an environmental chamber controlled by an automatic temperature controller (20–500 °C) in which the compartments were continuously purged with nitrogen. All samples were prepared by mixing with finely ground KBr as a 10% clay mixture. The sample was transferred to the diffuse reflectance cup positioned in the heating chamber, the surface levelled and a DRIFTS spectrum collected prior to any heating or purging treatment at 25 °C. The sample was purged with nitrogen for 15 min before collecting a second spectrum. The sample temperature was then raised at 25 °C increments to 500 °C allowing equilibration for 15 min at each temperature before each spectrum was recorded.

X-Ray diffraction traces were collected using a Philips PW1830 diffractometer operating at 35 kV and 45 mA with a copper target ($\lambda = 1.5418$ Å). A simple heating stage was used to collect diffraction profiles at different (increasing) temperatures (VT-XRD).[33]

Thermogravimetric analysis (TG) was performed using a Mettler TA3000 thermogravimetric analyser. The samples were preconditioned in a nitrogen gas flow for 15 min at 35 °C. The sample was then heated to 800 °C at a rate of 20° C min^{-1}. The traces were recorded as weight loss *versus* temperature but are presented as the negative of the first derivative (*i.e.* $-dw/dT$).

Evolved gas analysis was carried out using a synergic chemical analysis system supplied by Thermo Unicam.[34] This system consists of a thermobalance (TG131, Cahn) fitted with two outlets which are connected to heated transfer lines. One transfer line was connected to an infrared gas cell (10 cm path length) contained in an infrared (FTIR) spectrometer (Infinity Series, Mattson). The second transfer line was connected directly to a mass spectrometer (Automass System 2, Unicam). Thus, real-time TG–MS and TG–FTIR information was available.

Samples for X-ray fluorescence analysis were prepared by pressing powdered samples into cellulose before analysing the samples on a Philips PW2400 XRF spectrometer using calibration software prepared from standard reference materials.

2.3 Procedures

1.5 g of a kaolin sample was dispersed in 300 cm^3 of a 1 : 1 (v/v) distilled water : acetone mixture to which was added 2.75 g of phenylphosphonic acid. The reaction was carried out at 68 °C in a 500 cm^3 round-bottom flask fitted with a reflux condenser. The kaolin–PPA sample (KPPA) was treated for a period of five weeks, and the halloysite–PPA sample (HPPA) for one week. At the end of the reaction time the samples were subjected to five consecutive processes of centrifugation (at 4000 rpm) and washing with acetone. Finally, the solid white residue was allowed to dry in air at room temperature for 24 h. Phosphorus contents of digested samples were determined using ICP-AES by Medac, Brunel University, UK.

3 Results

Wypych and co-workers[26] explained that the topotactic reaction between kaolin and PPA resulted in the formation of covalent bonds between the acid and the clay surface according to the reaction:

$$Al_2Si_2O_5(OH)_4 + 3H_2O_3PPh \rightarrow Al_2Si_2O_5(OH)(HO_3PPh)_3{\cdot}2H_2O + H_2O$$

This implies that PPA reacts with all three of the inner surface hydroxyls and the only OH group remaining after the process is the relatively inaccessible inner sheet hydroxyl. The calculated weight percent of phosphorus in the above dihydrate is 13%. The phosphorus content of HPPA was 12.2% whereas for KPPA it was only 6.5%. Clearly, there was twice as much PPA in HPPA than in KPPA.

Fig. 1 shows how both kaolin (Fig. 1b) and halloysite (Fig. 1d) were expanded when phenylphosphonic acid was intercalated into the gallery increasing the layer spacing in both systems to 15.4 Å. This value agrees with that obtained by

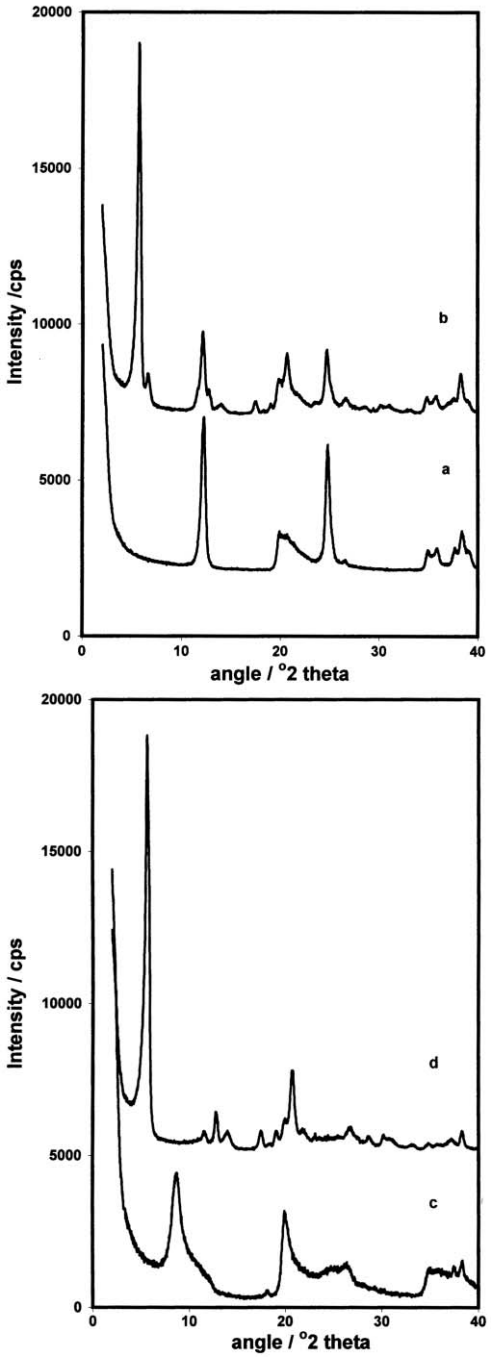

Fig. 1 X-Ray diffraction patterns for (a) kaolin, (b) kaolin–PPA, (c) halloysite and (d) halloysite–PPA.

others but no evidence of the reported higher spacing 16.45 Å intercalate was found.[26] The halloysite was completely expanded by the phenylphosphonic acid giving an intercalation ratio of 100% (Fig. 1d), whereas for kaolin–PPA (Fig. 1b) this ratio was only 82% (note the low intensity kaolin 001 peak at 12.3 ° 2θ for the KPPA intercalate). The intensity of the 001 peak for the phenylphosphonic acid intercalates varied little as the temperature was raised. The KPPA intercalation ratio was 70% after heating at 500 °C in air for 2 h. Clearly, the phenylphosphonic acid was strongly bound to the aluminol surface forming a well-ordered, thermally stable structure. Wypych and co-workers reported that heating their KPPA intercalates to 1000 °C resulted in the formation of crystalline $AlPO_4$ and SiO_2.[26,35] Semiquantitative XRF analysis of pressed powder samples of the KPPA prepared here confirmed that at least 75% of the original phosphorus content was present after heating at 500 °C for 2 h. Given that PPA alone decomposes at temperatures above 250 °C this represents a significant improvement in thermal stability as others have also found.[26,35]

The remarkable thermal stability of the PPA intercalates was also apparent from thermogravimetric analysis (Fig. 2). The derivative thermograms for halloysite and kaolin show that both minerals underwent dehydroxylation in the same temperature regime and reached a maximum, T_{max}, near 500 °C (Fig. 2a, c). Halloysite is distinguished from kaolin by the loss of interlayer water (12 wt%) with T_{max} at 75 °C. Both PPA intercalates exhibited two additional features. The first was a sharp maximum at 140 °C for KPPA (2.5 wt%) which occurred 10 °C higher for HPPA (5 wt%). Both these temperatures are similar to the value of 164 °C reported by others who attributed it to the loss of adsorbed water but provided no experimental evidence.[26] The second discriminating feature occurred, after layer dehydroxylation, at 585 °C in KPPA and at 610 °C in HPPA (Fig. 2b, d). Note that the intensity of the maximum occurring in the dehydroxylation region was very much less for HPPA than KPPA. Wypych and co-workers observed two endothermic peaks for the decomposition of their KPPA composites at 551 and 569 °C.[26] These temperatures agree closely with the values found by the present authors for kaolin from a different source (results not shown). Obviously, the temperature at which the PPA decomposes depends on the mineral used, provided that the two events were indeed separate processes of dehydroxylation and PPA decomposition.

Mass spectral analysis of the gases evolved during the decomposition of KPPA (Fig. 3) confirmed that the dehydroxylation process did indeed precede the decomposition of PPA in both intercalates. The intensity for the specific ion for water (m/z = 18) maximised near 150 and 500 °C, thus confirming that the desorption event near 150 °C was due to the loss of adsorbed water and that layer dehydroxylation preceded the major decomposition of PPA. Nonetheless, the specific ion chromatogram for benzene (m/z = 78), which was attributed to the loss of the phenyl ring from PPA, began at the same temperature as dehydroxylation but did not reach a maximum until over 100 °C later. The HPPA complex decomposed in a similar manner but the signal from the m/z = 18 ion near 150 °C was more intense (Fig. 3b), as anticipated due to the larger amount of adsorbed water (Fig. 2d), and significantly weaker in the dehydroxylation region.

The DRIFTS spectrum of HPPA obtained at 25 °C (Fig. 4a) exhibited a range of bands, most of which could be directly assigned to vibrations of the halloysite host or PPA. The bands at 3698 and 3625 cm^{-1} were assigned to the inner surface and inner sheet hydroxyls, respectively, the broader bands at 3551 and 3331 cm^{-1} were attributed to hydrogen bonded hydroxyls arising from either the interaction of water or PPA with the inner surface hydroxyls on the gibbsite sheet. In addition there was a broad contribution from hydrogen bonded OH in the region 2500–3700 cm^{-1} which diminished in intensity as the temperature was raised. The shoulder at 3076 together with the band at 3056 cm^{-1} were assigned to the C–H stretching vibrations of the phenyl ring. Other bands at 1591 and 1487 were also assigned as phenyl ring vibrations. Phenyl ring bands at 749, and 693 cm^{-1} overlapped with kaolin/halloysite bands. The assignment of the broad band at 1643 cm^{-1} to hydrogen bonded water was confirmed by its poor thermal stability (*vide infra*). The P–C stretch was clearly evident at 1439 cm^{-1} and remained virtually unaltered (up to 500 °C) as the sample temperature was raised, supporting the evidence above that PPA did not decompose until >500 °C. There was some uncertainty regarding the band at 1207 cm^{-1} because the ν(P=O) stretch occurs at 1220 cm^{-1} in PPA. The same was true of the 1140 cm^{-1} ν(P–O) stretching band which was also downshifted (by 26 cm^{-1}) and appeared at 1164 cm^{-1}. The other ν(P–O) bands at 1068, 1040 and 990 cm^{-1} were obscured

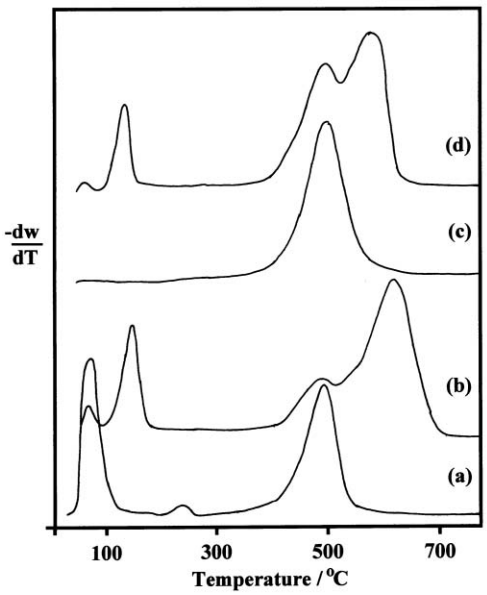

Fig. 2 Derivative thermograms for (a) halloysite, (b) halloysite–PPA, (c) kaolin and (d) kaolin–PPA.

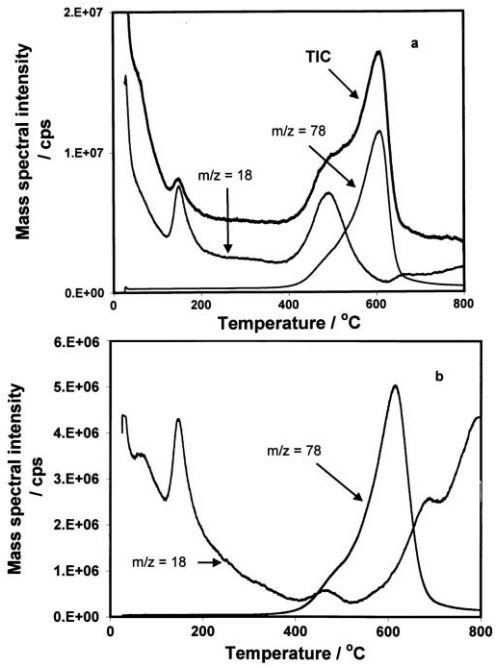

Fig. 3 TG–MS traces for the desorption of water (m/z = 18) and benzene (m/z = 78) from (a) kaolin–PPA and (b) halloysite–PPA (TIC = total ion chromatogram).

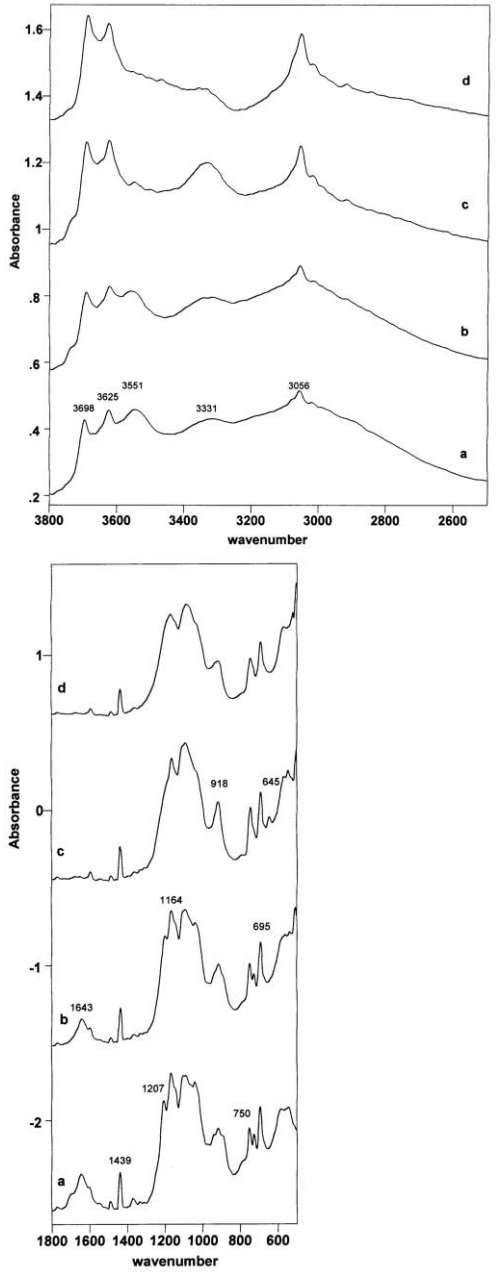

Fig. 4 Variable temperature DRIFTS spectra of the halloysite–PPA intercalate at (a) 25 °C, (b) 100 °C, (c) 125 °C and (d) 225 °C.

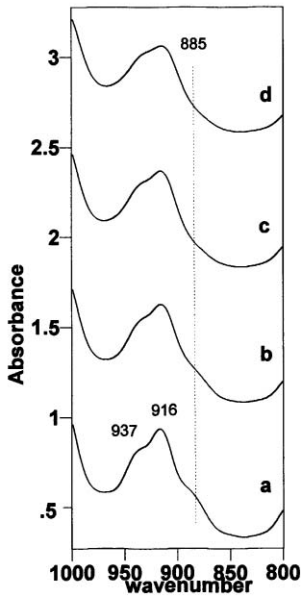

Fig. 5 Variable temperature DRIFTS spectra (OH deformation region) of the halloysite–PPA intercalate at (a) 25 °C, (b) 100 °C, (c) 125 °C and (d) 225 °C.

by the Si–O stretching bands. Finally, halloysite has two OH deformation bands at 916 and 934 cm^{-1} assigned to the inner sheet and inner surface hydroxyls, respectively. However, there was clearly a third contribution in this spectral region near 885 cm^{-1} (Figs. 4a and 5a). The inner sheet hydroxyl is considered to be relatively inaccessible although its perturbation *via* interaction with sorbed hydrazine has been reported[16] which suggests that the 885 cm^{-1} band may represent a significant downward shift in the 934 cm^{-1} band.

The spectrum recorded at 100 °C (Fig. 4b) showed that a small quantity of adsorbed water had been removed in that the relative intensity of the 1643 cm^{-1} band had been reduced in comparison to the 1439 cm^{-1} band, causing the shoulder at 1598 cm^{-1} to become better resolved. The 1207 cm^{-1} band had shifted downwards in frequency but was still visible on the high wavenumber side of the main SiO vibrational envelope. The three poorly resolved bands in the 880–950 cm^{-1} (Figs. 4b and 5b) region were now less distinct from each other. At 125 °C the bands at 3547 and 1642 cm^{-1} had been removed, the 1205 cm^{-1} band had merged completely with the main SiO vibration and the 885 cm^{-1} band had essentially disappeared leaving the bands at 937 and 916 cm^{-1}. In addition, the broad band attributed to hydrogen bonded OH in the 2500–3700 cm^{-1} region was significantly reduced whilst the 3331 cm^{-1} band became very prominent and remained so as the temperature was raised but gradually diminished in intensity. The bands for the P–C stretch (1437 cm^{-1}) and the phenyl ring vibrations (3056, 1596, 1487 cm^{-1}) were not significantly affected as the temperature was increased but the 724 cm^{-1} band was no longer visible at 125 °C and a new band appeared at 645 cm^{-1}. This band, which has not been assigned, was still present at 200 °C but not at 225 °C.

Clearly, significant spectral changes occurred in the temperature range 100–225 °C when the TG–MS data (Fig. 3) showed that appreciable amounts of water were being desorbed. Broadly similar observations were recorded in the VT-DRIFTS spectra for KPPA although there were differences in the detail. The P–C stretch and ring vibrations were thermally stable but no 645 cm^{-1} band was observed when the 724 cm^{-1} band disappeared. The 1204 cm^{-1} band merged with the main SiO vibration between 125 and 150 °C when the bands at 3544 and 1642 cm^{-1}, attributed to sorbed water, were reduced to zero. The band near 3330 cm^{-1} was present up to 225 °C but was not as prominent as in the corresponding spectra for HPPA (Fig. 4b, c). Finally, the band at 885 cm^{-1} was less intense than in the HPPA spectra and was removed by 150 °C.

4 Discussion

Calculations based on the phosphorus contents of HPPA (12.2%) and KPPA (6.5%) indicate that the formulae for the two complexes are $Al_2Si_2O_5(OH)(HO_3PPh)_3{\cdot}5H_2O$ and $Al_2Si_2O_5(OH)_3(HO_3PPh){\cdot}3H_2O$, respectively, within the accuracy of determining the water content of the samples from thermogravimetry. The stoichiometry of the HPPA complex suggests that three of the four available hydroxyls should be removed. This is qualitatively supported by the marked reduction in the weight loss attributed to layer dehydroxylation of HPPA (Fig. 2b) when compared with halloysite alone (Fig. 2a) and the corresponding TG–MS data (not illustrated). In contrast, only one of the four hydroxyls should be removed in KPPA which appears to be the case given that a substantial

weight loss occurs in the dehydroxylation region (Figs. 2c, d and 3). This means that the 26% weight loss in HPPA above 420 °C can be divided into 3.5%, due to dehydroxylation, and 22.5%, due to loss of organic species. The corresponding figures for the 21% loss from KPPA are 10.5%, due to dehydroxylation, and 10.5%, from the desorption of organic species. This approach is considered to be qualitatively correct because the weight loss attributed to the loss of organic matter is in line with the phosphorus contents of the two intercalates. The marked difference in these values reinforces the ease with which halloysite can accommodate interlayer species compared with kaolin, and that more PPA molecules occupy the gallery in halloysite than in the kaolin used here. Nonetheless, the weight loss values are lower than the 40% reported by others[26] and also serve to illustrate that the intercalation ratio can be misleading regarding the amount of sorbed species. It is important not to confuse the number of expanded layers with the number of molecules actually present in the gallery.

The expansion of the interlayer spacing by 8 Å is consistent with the phenyl ring of PPA being oriented at a high angle to the kaolin basal surface. Halloysite adsorbs more PPA than kaolin and requires only one week, as opposed to five, in order to achieve this loading. Alberti *et al.*[30] reported that the rate of the topotactic reaction between γ-zirconium phosphate and PPA was much faster in a water–acetone mixture than in water alone. They attributed the difference to the presence of exfoliated layers in the mixed solvent system which permitted PPA easy access to the reaction sites, whereas in water (where no exfoliation occurred) the progress of the topotactic reaction was diffusion limited. The presence of exfoliated halloysite layers would provide a logical explanation for the relative speeds of the topotactic reactions reported herein.

It is common practice when studying kaolin and halloysite to report the intercalation ratio which provides a measure of the number of expanded *versus* non-expanded layers. However, it is important not to confuse the number of expanded layers with the number of molecules actually present in the gallery. Frost *et al.*[12] have recently reinforced the observation that the intensity of the OH stretching modes of the inner surface hydroxyls are a more quantitiative measure of the number of interlayer OH groups which are involved in interactions with adsorbed molecules in the gallery. For example, when one molecule of DMSO interacts with each inner surface hydroxyl in kaolin the bands at 3695, 3668 and 3652 cm^{-1} (*vide infra*) diminish to almost zero intensity. Consequently, the residual intensity at 3695 cm^{-1} in both KPPA and HPPA confirmed that some inner surface hydroxyls had not been replaced and were not interacting with PPA. It was not possible to observe the regeneration of the OH stretching band as the PPA degraded because its remarkable thermal stability means that it does not decompose/desorb until above the maximum operating temperature of the VT-DRIFTS accessory.

Low defect, well-crystallised kaolin has four distinct OH stretching vibrations, at 3695, 3668, 3652 and 3620 cm^{-1}. The first three are assigned to the inner surface hydroxyls available for interaction with molecules occupying the kaolin gallery. The fourth, at 3260 cm^{-1}, is assigned to the inner sheet hydroxyl where the tetrahedral and octahedral sheets are joined. This inner sheet hydroxyl is generally considered to be unavailable for interaction with adsorbed molecules, although its perturbation by sorbed hydrazine has been reported.[16] The OH stretching region of halloysite generally contains two distinct peaks at 3695 and 3620 cm^{-1}. The presence of water in the interlayer reduces the intensity and broadens the 3695, 3668 and 3652 cm^{-1} bands.

Monomeric, non-hydrogen bonded water in the vapour phase has bands at 3755 and 1595 cm^{-1}. These bands occur at 3455 and 1645 cm^{-1} in liquid water and at 3255 and 1655 cm^{-1} in ice. The OH stretching modes for weakly hydrogen bonded water occur in the 3500–3590 cm^{-1} region and below 3420 cm^{-1} for strongly hydrogen bonded water. Frost *et al.*[12] have stated that as the OH stretching frequency decreases, the HOH bending frequency increases thus providing a measure of the strength of the bonding of water molecules either physically or chemically bonded to the kaolin surface (for example). Bending frequencies below 1630 cm^{-1} indicate weak hydrogen bonding whereas frequencies above 1650 cm^{-1} indicate coordinated and chemically bound water. Thus, the loss of the bands at 3550 and 1640 cm^{-1} (Fig. 4c), together with the loss of water confirmed by TG–MS, indicate the loss of water which was weakly hydrogen bonded to the surface aluminols or any OH groups remaining on PPA. The band at 3330 cm^{-1} suggests a more strongly hydrogen bonded species which agrees with its greater thermal stability. It is not clear at this point why there was no associated OH bending mode near 1640 cm^{-1}.

Frost *et al.*[12] have used DRIFTS to study the interaction of DMSO with the inner surface hydroxyls of kaolin and reported the loss of the bands at 3695, 3668 and 3652 cm^{-1} together with the appearance of new bands at 3660, 3538 and 3502 cm^{-1}. These new bands were assigned to hydrogen bond formation between the S=O bond of DMSO and the inner surface hydroxyls (3660 cm^{-1}), water involved in bonding to the inner surface hydroxyls (3538 cm^{-1}) (thus confirming the assignment above) and water hydrogen bonded to lone pairs of electrons on the sulfur atom in DMSO (3502 cm^{-1}). The authors did not report VT-DRIFTS data but associated TG–MS results confirmed that water was occluded in the kaolin–DMSO complex and that it was desorbed at 70 °C. Tunney and Detellier[24] reported bands at 3575 and 3394 cm^{-1} when they grafted ethylene glycol on to the inner surface OH groups of kaolin. These two bands were assigned to the stretching of the surface OH groups and the OH group of ethylene glycol involved in the hydrogen bonding, respectively. All of these bands are at a higher wavenumber than the thermally stable, prominent 3330 cm^{-1} band observed in HPPA (Fig. 4) and to a lesser extent in KPPA. The 3330 cm^{-1} band gradually decreased in intensity as the sample temperature was raised. Thermogravimetry showed that the sample lost 3 wt% during this temperature interval (200–400 °C) and only water (m/z = 18) was identified using TG–MS. Therefore, given that the 3330 cm^{-1} band was more intense in HPPA than in KPPA and that the former contains twice the amount of PPA, the 3320 cm^{-1} band was assigned to water hydrogen bonded to the phosphonic acid moiety of PPA.

Frost's group have reported a deformation band at 905 cm^{-1} in the room temperature DRIFTS spectrum when formamide[12,15] or DMSO[14] are present in the kaolin gallery, and have attributed it to the result of hydrogen bonding between the C=O or the S=O group to the surface aluminols. OH deformation bands as low as 885 cm^{-1} have been reported in the presence of hydrazine[19] but it is uncertain whether this band should be attributed to a perturbed inner sheet hydroxyl or an inner surface hydroxyl perturbed by a weak hydrogen bond (with an associated hydroxyl stretching band at 3626 cm^{-1}). However, the fact that the 885 cm^{-1} band observed herein was lost at the same temperature as the bands at 1643 and 3547 cm^{-1} (in both HPPA and KPPA) favours the interpretation that it arises from water weakly hydrogen bonded to the inner sheet hydroxyls.

5 Conclusions

Halloysite adsorbed twice as much PPA as kaolin in a much shorter time. Both PPA intercalates formed an expanded phase which exhibited remarkable thermal stability. The PPA moiety decomposed *via* loss of the phenyl ring at temperatures above which layer dehydroxylation had ended. Complementary TG–MS and variable temperature DRIFTS data showed that the

HPPA and KPPA complexes retained water in two different environments within the intercalates. The first (3547 and 1643 cm^{-1}) was weakly hydrogen bonded to the inner surface hydroxyls and was lost during the sharp maximum in the DTG (Figs. 2 and 3) The second (3330 cm^{-1}) was desorbed more gradually as the temperature increased giving rise to the TG–MS signal for $m/z = 18$ (Fig. 3) between 200 and 400 °C.

References

1 R. F. Giese, in *Hydrous Phyllosilicates*, ed. S.W. Bailey, Mineralogical Society of America, Washington, DC, 1988, p. 29.
2 D. L. Bish, *Clays Clay Miner.*, 1993, **41**, 738.
3 M. Cruz, H. Jacobs and J. J. Fripiat, *Proc. Int. Clay Conf.*, 1973, 35.
4 R. F. Giese, *Clays Clay Miner.*, 1978, **26**, 31.
5 R. F. Giese, *Bull. Miner.*, 1982, **105**, 417.
6 K. J. Range, A. Range and A. Weiss, 'Experimental Classification of Kaolin–Halloysite minerals', in *Proceedings of the International Clay Conference*, Tokoyo, Japan, ed. L. Heller, Israel University Press, Jerusalem; *Proc. Int. Clay Conf.*,1969, **1**, 3.
7 S. W. Bailey, in *Proceedings of the International Clay Conference*, Strasbourg, France, ed. V. C. Farmer and Y. Tardy; *Sci. Geol. Mem.* 1989, **86**, 89.
8 G. J. Churchman, J. S. Whitton, G. G. C. Claridge and B. K. G. Theng, *Clays Clay Miner.*, 1984, **32**, 214.
9 G. J. Churchman and B. K. G. Theng, *Clay Miner.*, 1984, **19**, 161.
10 C. J. Johnstone, G. Sposito, D. F. Spocian and R. R. Birge, *J. Phys. Chem.*, 1984, **88**, 5859.
11 J. G. Thompson and C. Cuff, *Clays Clay Miner.*, 1985, **33**, 490.
12 R. L. Frost, J. Kristof, G. N. Paroz and J. T. Kloprogge, *J. Phys. Chem. B*, 1998, **102**, 8519.
13 S. Olejnik, A. M. Posner and J. T. Quirk, *Clays Clay Miner.*, 1974, **19**, 83.
14 R. L. Frost, J. Kristof, E. Horvath and J. T. Kloprogge, *Spectrochim. Acta, Part A*, 2000, **56**, 1711.
15 R. L. Frost, J. Kristof, E. Horvath and J. T. Kloprogge, *Spectrochim. Acta*, 2000, **56**, 1191.
16 C. T. Johnston and D. A. Stone, *Clays Clay Miner.*, 1990, **38**, 121.
17 R. L. Frost, J. Kristof, G. N. Paroz and J. T. Kloprogge, *J. Colloid Interface Sci.*, 1998, **208**, 216.
18 R. L. Frost, J. T. Kloprogge, J. Kristof and E. Horvath, *Clays Clay Miner.*, 1999, **47**, 732.
19 C. T. Johnstone, D. L. Bish, J. Eckert and L. A. Brown, *J. Phys. Chem. B*, 2000, **104**, 8080.
20 Y. Sugahara, S. Satokawa, K-I. Yoshioka, K. Kuroda and C. Kato, *Clays Clay Miner.*, 1989, **37**, 143.
21 M. Makoto, *Clays Clay Miner.*, 1999, **47**, 793.
22 Y. Komori, Y. Sugahara and K. Kuroda, *Appl. Clay Sci.*, 1999, **15**, 241.
23 S. Olejnik, A. M. Posner and J. T. Quirk, *Clay Miner.*, 1970, **8**, 421.
24 J. J. Tunney and C. Detellier, *Chem. Mater.*, 1993, **5**, 747.
25 J. J. Tunney and C. Detellier, *Clays Clay Miner.*, 1994, **42**, 552.
26 J. L. Guimarãs, P. Peralta-Zamora and W. J. Wypych, *J. Colloid Interface Sci.*, 1998, **206**, 281.
27 L. Raki and C. Detellier, *Chem. Commun.*, 1996, 2475.
28 H. Nijs, A. Clearfield and E. F. Vansant, *Microporous Mesoporous Mater.*, 1998, **23**, 97.
29 O. L. Alves and M. F. Vichi, *J. Mater. Chem.*, 1997, **7**, 1631.
30 G. Alberti, E. Giontella and S. Murcia-Mascaros, *Inorg. Chem.*, 1997, **36**, 2844.
31 K. Sakamoto, Y. Tsunawaki, A. Nakahira, K. Kitahama, J. Ichihara and S. Yamaguchi, *Nanostruct. Mater.*, 1999, **12**, 491.
32 R. L. Frost, *Clays Clay Miner.*, 1998, **46**, 280.
33 G. Brown, B. Edwards, E. C. Ormerod and A. H. Weir, *Clay Miner.*, 1972, **9**, 407.
34 C. Breen, P. M. Last and M. Webb, *Thermochim. Acta*, 1999, **326**, 151.
35 J. L. Guimares, C. Jorge de Cunha and F. Wypych, *J. Colloid. Interface Sci.*, 1999, **218**, 211.